

Article

Potential Sea Level Rise Impacts in Acapulco Diamante, Mexico

Ramiro Salvador Gómez-Villeras^{1,*} , Adalberto Tejeda-Martínez², Ana Cecilia Conde Álvarez³, Maximino Reyes Umaña¹, José Luis Rosas-Acevedo¹, Manuel Ignacio Ruz Vargas⁴ and Erick Alfonso Galán Castro¹

¹ Centro de Ciencias de Desarrollo Regional, Universidad Autónoma de Guerrero, Acapulco 39640, Mexico; 11471@uagro.mx (M.R.U.); jlrosas@uagro.mx (J.L.R.-A.); erick.galan@conacyt.mx (E.A.G.C.)

² Ciencias Atmosféricas, Universidad Veracruzana, Xalapa 91090, Mexico; atejeda@uv.mx

³ Instituto de Ciencias de la Atmosfera y Cambio Climático, Universidad Nacional Autónoma de México, Mexico City 04510, Mexico; conde@unam.mx

⁴ Facultad de Arquitectura y Urbanismo, Universidad Autónoma de Guerrero, Chilpancingo 39000, Mexico; maruz@uagro.mx

* Correspondence: rsgomez@uagro.mx; Tel.: +52-(744)-587-9302

Abstract: The potential impacts of sea level in the study region are presented using the Integrated Procedure for Estimate Sea Level Impacts (IPESLI), made up of Landsat images, official databases, and design software for geographic information systems. IPESLI is useful in areas with little georeferenced and validated information. The sea level projections are based on the climate projections, which incorporate the possible attenuation of the ice sheet near the upper end of Antarctica. Flood risk statistics were used to simulate the frequency of extreme flooding across the planet. The IPESLI was calibrated using seven field visits to compare the height values generated by the digital elevation model against the in situ data. The inundation maps generated in the study can be used to find the most vulnerable areas and initiate decision making for coastal adaptation. The IPESLI procedure has the potential to contribute to the formation of a communication bridge between climate change science and policy makers. The projection is profound for all scenarios, but it is particularly devastating for the Acapulco Diamante area if we start with the worst future climate scenario (SSP5-RCP8.5).

Keywords: sea level rise; coastal zones; climate change; SSP-RCP; flooding risk



Citation: Gómez-Villeras, R.S.; Tejeda-Martínez, A.; Conde Álvarez, A.C.; Reyes Umaña, M.; Rosas-Acevedo, J.L.; Ruz Vargas, M.I.; Galán Castro, E.A. Potential Sea Level Rise Impacts in Acapulco Diamante, Mexico. *Climate* **2022**, *10*, 45. <https://doi.org/10.3390/cli10030045>

Academic Editors: Antonino Marvuglia, Mainer Llaguno-Munitxa and Federico Amato

Received: 26 January 2022

Accepted: 15 March 2022

Published: 19 March 2022

Publisher's Note: MDPI stays neutral with regard to jurisdictional claims in published maps and institutional affiliations.



Copyright: © 2022 by the authors. Licensee MDPI, Basel, Switzerland. This article is an open access article distributed under the terms and conditions of the Creative Commons Attribution (CC BY) license (<https://creativecommons.org/licenses/by/4.0/>).

1. Introduction

The forecast of populations in low-elevation coastal areas began at more than 680 million people in 2010 and will possibly exceed 1000 million by 2041–2060 [1]. As global temperatures rise, rising sea levels will threaten the lives and property of societies in coastal regions, creating economic, social, and environmental problems and increasing the frequency and intensity of coastal flooding [2]. Therefore, it is essential to estimate sea level rise by the end of this century under different global warming conditions.

The average sea level increased 20 cm between 1901 and 2018, with an annual average of 1.3 mm between 1901 and 1971, increasing to 1.9 mm between 1971 and 2006 and 3.7 mm between 2006 and 2018. Human influence is the most likely cause of such increases [3]. The Paris Agreement proposed limiting future temperature increase to 1.5 °C compared to the second half of the nineteenth century so as to reduce the impacts of climate change [4]. Since the Fourth Assessment Report (AR4) of the Intergovernmental Panel on Climate Change (IPCC), progress has been made in observing the average changes in sea level and the different components that contribute to it [1,3,5]. Total sea level rise is about 3 mm per year (about one-eighth of an inch per year). About one-third comes from Greenland and Antarctica, one-third from glaciers, and one-third from the expansion of seawater as it warms [6,7].

Long-term models have sparked debate about the possibility of future sea level increases that are more significant than the IPCC's projections [3,5,8,9]. Policymakers,

planners, coastal engineers, and civil society need clear sea level rise projections for risk assessment and decision making [10]. The problem is more complex if it is addressed at the regional level: “Regional Relative Sea Level = Short-Term Effects + Sterodynamic Variability + Glaciers + Land Water Storage + Ice Sheets + Subsidence” [11]. The absence of this type of projection at the regional level has meant an evident lack of concern about the problem of climate change in local governments, which has been detected by civil actors trying to influence political agenda in this regard [12].

Studies predicting the contribution of the Antarctic ice sheet to sea level rise show that by 2081–2100 [13], the sum of the components of global sea level rise will exceed 1.5 m. According to Mastrandrea et al. (2011), the level of confidence assigned to research depends on the line of evidence that provides information for research and its degree of consistency [14]. Hinkel et al. (2019) state that coastal communities need to understand the expected changes in the height and frequency of extreme sea level events (ESL) in order to select appropriate and cost-effective adaptation strategies [10]. Medium-term decisions (30 years) include flood control and other infrastructure and spatial planning decisions.

Coastal protection infrastructure, such as levees and breakwaters, involves making decisions that span 30 to 100 years or even longer [15]. Critical protective infrastructure, such as wind barriers, requires decades of planning and implementation, so its lifespan must be even longer [16]. That is, in this sector of decision making, horizons of more than 100 years must be considered if a long-term critical infrastructure is planned [17]. Land-use planning, coastal zone risk zoning, and coastal adjustment decisions [18] should be considered to last as long as a century. Representative Concentration Pathways (RCPs) describe different levels of greenhouse gases (GHGs) and other radiative emissions that could occur in the future. The four pathways encompass a wide range of climate system forcings between 2081 and 2100—2.6, 4.5, 6.0, and 8.5 watts per square meter (W/m^2)—but these are not accompanied by any socioeconomic “narrative” [19,20].

Socioeconomic factors that will be relevant over the next century include population, economic growth, education, urbanization, and the pace of technological development [21]. The Shared Socioeconomic Pathways (SSPs) examine five ways in which the world would evolve in the absence of climate policies and how different levels of climate change mitigation could be achieved when the mitigation objectives of the RCPs are combined with the SSPs [22]. Both routes are complementary. The RCPs set the trajectories of the greenhouse gas concentrations and the magnitudes of radiative forcings that could occur by the end of the century; the SSPs establish the context in which emission reductions will (or will not) be achieved [23], particularly in coastal zones.

The preceding studies have shown the need to display data that is under large uncertainties, both with respect to the understanding of climate change and as a tool for decision makers [24], particularly in coastal zones. Over the past four decades, elevation, specifically Digital Elevation Models (DEMs), have been used to identify low-lying coastal areas [25–27]. Previous research has shown that the quality of the data, and the transformations to which they are subjected, influence the correct modeling of future impacts [28–30].

The present work aimed to use recent satellite images to extract a digital elevation model of the study area through the sea level projections of Kopp et al. (2017) and the flood probability statistics of Muis et al. (2016). Three different coastal flood scenarios were generated: SSP1-RCP2.6 for the sustainable pathways, SSP2-RCP4.5 for moderate commitment, and SSP5-RCP8.5 for fossil fuel-rich development [31,32].

This work is based on the fact that Mexico in general, and Acapulco in particular, is following a pathway that is not committed to future economic and social development [33], with little investment in education or health at the national level, driven by an economy based on fossil fuels and high energy consumption, along with rapid growth of the population, persistent inequality, and poverty [34,35]. It represents a heterogeneous state with a continuously increasing population and a plan of economic growth oriented towards mass tourism, which is more fragmented and slow than in other areas [36].

Study Area

Acapulco is a Mexican city and port located in the state of Guerrero, on the south coast of the country, 379 km by road from Mexico City [37]. It is the largest city in the state, with 658,609 inhabitants, and is the municipality with the largest population, with 779,566 denizens [38]. The general location of Acapulco within the Mexican Republic, and the location of the study area, are shown in Figure 1.

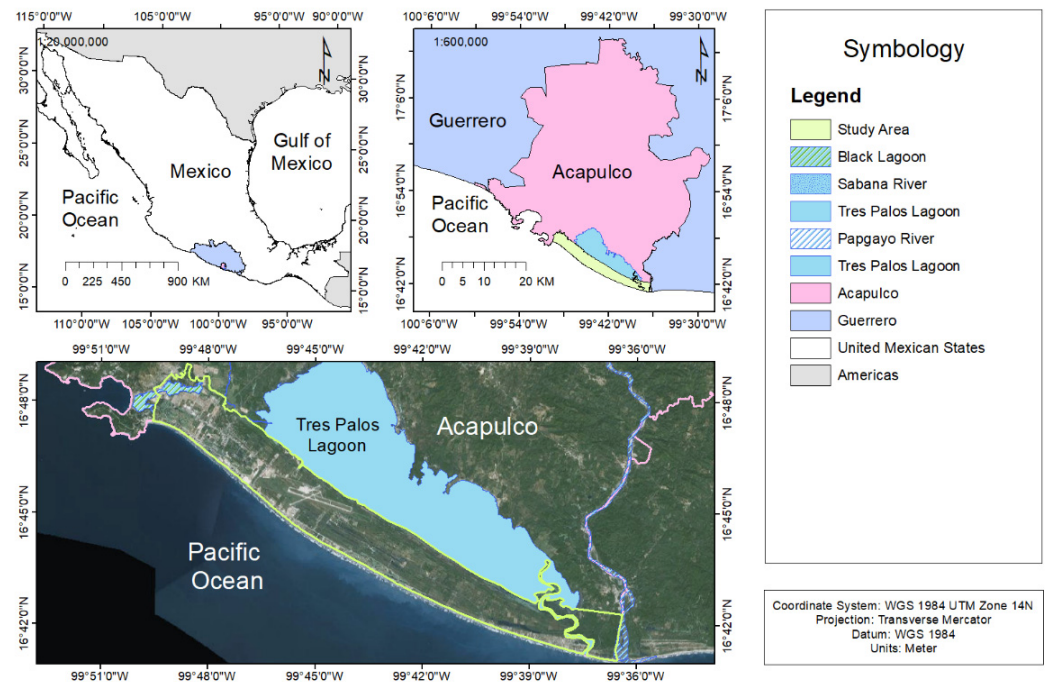


Figure 1. Location of the state of Guerrero in the Mexican Republic (above-left) and the municipality of Acapulco delimitation of the study area (above-right), and the limits of the study area in their true colors (below). Bands 2, 3, 4 for Landsat 8 (1, 2, and 3 for older Landsats).

Acapulco is one of Mexico's top tourist destinations [39]. It has a coastline approximately 62 km long (12.3% of the coast of the state of Guerrero), and it exhibits a high level of environmental deterioration. From 2010 to 2015, the state of Guerrero lost 17.8% of its mangrove areas, equivalent to 1448 ha [40]. In 1921, the municipality of Acapulco was inhabited by 5768 people; by 1950, there were 55,892 inhabitants [41]; by 2010, there were 789,971 [42]; and the 2020 census recorded a population of 779,566 inhabitants, that is, about 10,000 inhabitants fewer than a decade earlier.

The city comprises three large tourist areas [43]: Acapulco Tradicional, Acapulco Dorado, and Acapulco Diamante (Figure 2). Each area was developed in different eras: the Acapulco Tradicional is the central area of the city and the historical point of origin of its urban environment. Acapulco Dorado was created in the 1950s, and Acapulco Diamante arose at the end of the 1980s. The geographical boundaries of the study area are specified in Table 1. The boundaries of the study area within the Acapulco Diamante zone are shown in Figure 1 and are as follows:

- To the north, the lagoon of Tres Palos (also known as Nahualá);
- To the east, the Papagayo River;
- To the south, the Pacific Ocean;
- To the west, the Black Lagoon.

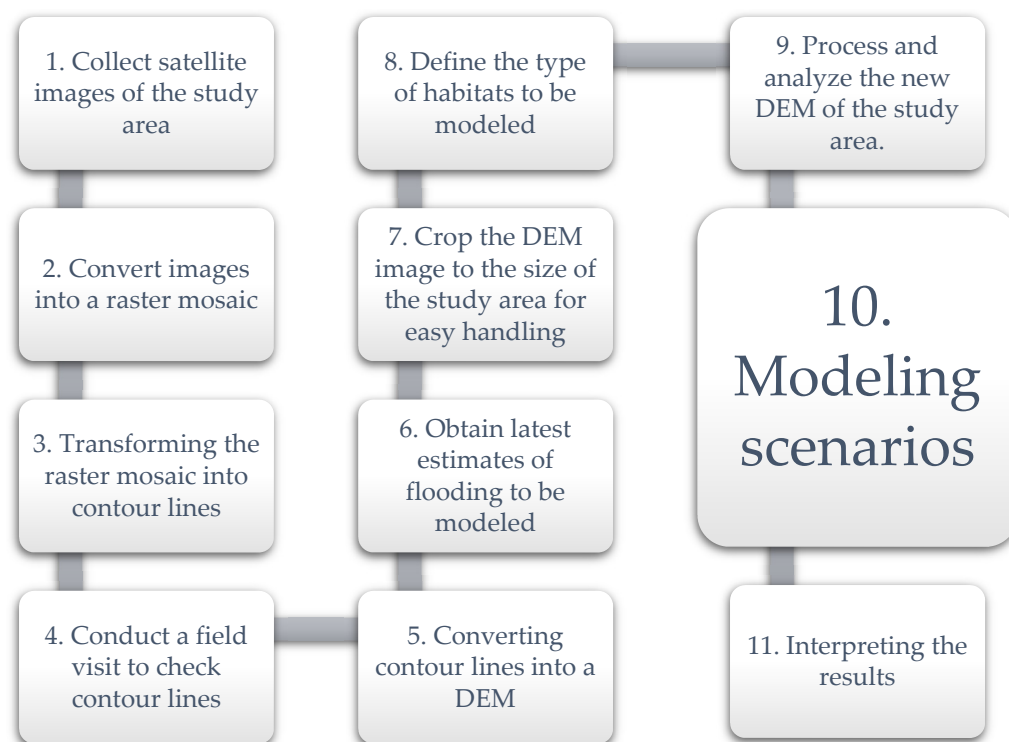


Figure 2. The Integrated Procedure for Estimate Sea Level Impacts (IPESLI), applied to estimate the effects of sea level rise in coastal areas.

Table 1. Geographical boundaries of the study area.

North	South	East	West
16.817829	16.683274	−99.604305	−99.828557

The coastal area of the municipality of Acapulco has historically been very vulnerable to hydrometeorological phenomena [44]. It is exposed to coastal flooding by tropical storms, as occurred with hurricane Henriette in 1995 [45], hurricane Paulina in 1997 [46], and hurricanes Ingrid and Manuel in 2013 [47,48].

Thanks to the infrastructural improvement, mainly due to the investment in tourism promotion programs in the Diamante area, the development of housing has caused a constant increase in population density in this area, which has increased the population at risk of coastal flooding [49,50]. Despite being one of the most valuable areas in the city, it is also a high-risk area [51]. The Diamante Zone is home to about a quarter of the municipality's population and comprises a quarter of the urban infrastructure [52].

The Atlas of Natural Hazards of the City of Acapulco [53] identifies sites with severe problems of pluvial flooding, especially towards the eastern part of the city in the areas adjacent to the Laguna de Tres Palos. Another area that has been identified is located between the Black Lagoon and the Pacific Ocean. Both areas are flat, which increases the difficulty of draining the excess water from bottlenecks of natural channels and parts of the Acapulco Diamante zone.

However, even though Acapulco is the largest city in Guerrero, it currently lacks a proposal for the reduction of risk due to sea level rise, which has been validated and endorsed by social actors [42]. Although there have been institutional efforts to assess risk, action has not been taken [46].

2. Materials and Methods

In this work, estimates of future sea level rise based on the climate projections constructed by Kopp et al. (2017) have been made by adding the possibility of the early decline

of the West Antarctic ice sheet [31,54] with different ranges of future sea level rise under different climate change scenarios. We used the flood risk statistics published by Muis et al. (2016), who studied 35 years of global atmospheric condition records to simulate and estimate the frequency of extreme flooding around the world [31,32].

For their global sea level rise projections, Kopp et al. (2017) assume that there is independence among sea level contributors, so they use expert judgment for correlation of uncertainty in the projections, which shows that with RCP 8.5, by 2100, at the 99.5th percentile of their sea level projection, it increased from 176 cm (their uncorrelated hypothesis) to 187 cm (with the expert correlation) [31]. This shows the effect of the correlation structure for the tail of the future sea level distribution. It is essential to broaden the range of the probabilities at stake, because low probability events are also important for risk management assessment, as long as they have a high impact [55].

The IPCC Group 1 Sixth Assessment Report (from now on, AR6W1) provides projections of sea levels and their uncertainty [3]. The AR6W1 projections of sea level rise are based on the following SSP-RCPs: SSP1-RCP2.6 for sustainable pathways, SSP2-RCP4.5 for a moderate commitment, and SSP5-RCP8.5 for fossil fuel-rich development. For physical reasons, the instability of the sea ice sheet, the detachment of glaciers, and the thermal expansion of the oceans all place an upper limit on sea level rise by 2081–2100 [56]. Recent projections can be used to assess this limit. Related studies show global consensus on a projected increase of between 2 and 4 m by 2081–2100, in relation to the values pertaining to the beginning of this century [57].

The here-presented *Integrated Procedure for Estimate Sea Level Impacts* (IPESLI) integrates Landsat images, official databases, and design software for geographic information systems. IPESLI is useful in areas with little georeferenced and validated information (Figure 2). Table 2 presents the projected values of global warming for 2041–2060, 2061–2080, and 2081–2100, relative to the base values of 1995–2014 [3]. Using the NASA Sea Level Projection Tool, we are able to visualize the local projection data from the IPCC 6th Assessment Report (AR6) [58].

Table 2. Sea level increase in centimeters for scenarios (A) Optimistic SSP1-RCP2.6, (B) Conservative SSP2-RCP4.5, and (C) Extremist SSP5-RCP8.5, concerning the average values for 1995–2014 [31]. The sea level projections are based on the climate projections made by Kopp et al. (2017).

Optimistic SSP1-RCP2.6		
Year	Elevation (m)	
2041–2060	0.41	(A)
2061–2080	0.67	
2081–2100	0.98	
Conservative SSP2-RCP4.5		
Year	Elevation (m)	
2041–2060	0.43	(B)
2061–2080	1.04	
2081–2100	1.58	
Extremist SSP5-RCP8.5		
Year	Elevation (m)	
2041–2060	0.48	(C)
2061–2080	1.15	
2081–2100	2.43	

The IPCC's projections of future sea level rise are derived from models based on different processes [3]. Ocean warming causes thermal water expansion, the melting of high mountain glaciers and polar ice caps in Greenland and Antarctica, increases in the amount of groundwater extracted, and contributions of continental surface water. We believe the local projections underestimate the sea level rise in the study area; therefore, the

projections used in our scenarios are based on three pairs of SSP-RCPs adapted from the climate projections constructed by Kopp et al. 2017 [31].

The three scenarios of sea level rise employed in this paper (Table 2) are described below.

- A. Optimistic scenario: SSP1-RCP2.6 is a “rigorous” approach. According to the IPCC, SSP1-RCP2.6 requires that carbon dioxide (CO₂) emissions begin to decline in 2020 and reach zero by 2081–2100, consistent with the 1.5 °C warming cap, a target of the Paris Agreement. It implies 840 gigatons of total net carbon pollution by 2081–2100.
- B. Conservative scenario: SSP2-4.5 emissions will peak around 2040 and then decline to half the 2041–2060 level by 2081–2100. This implies approximately 2 °C of warming from the 1850–1900 level and 1266 gigatons of total carbon pollution by 2081–2100.
- C. Extremist scenario: In SSP5-8.5, emissions continue to increase throughout the 21st century. RCP8.5 is considered the basis of the worst-case climate change scenario, and the result is an overestimation of projected coal production. This scenario is named “Extremist” in this study. It involves 3 or 4 °C of heating and 2430 gigatons of carbon dioxide equivalent emissions by 2081–2100.

Different datasets were obtained from sources such as digital images, cartography, and field data for the area of Acapulco Diamante and its coast [59]. Cartographic information on coastal water bodies (e.g., Laguna de Tres Palos) [60] and the outline of the coast (e.g., inner rim and coast) were obtained from the National Institute of Statistics and Geography (from now on, INEGI) [61]. USGS Earth Explorer is a platform containing one of the largest databases of specialized information from various remote sensing satellites. A shapefile of the study area was used to define the region of interest, which is the geographic boundary that restricts the search in order to acquire data. A shapefile of the study area was delimited between 2019 and 2020. We selected L8 OLI/TIRS and L7 ETM + [62].

Table 3 lists the extracted images, the satellite from which they were taken, and their respective dates. Spatial resolution refers to the size of a pixel on the ground. Landsat data have a 50 m resolution, meaning that each pixel represents an area of 50 m × 50 m above the ground [59].

Table 3. General characteristics of the satellite images used in this study.

Path/Row	Sensor Landsat	Date
26/48	LS5-TM	3 April 2019
26/48	LS7-ETM+	8 October 2019
26/48	LS7-ETM+	1 December 2019
26/48	LS8-OLI/TIRS	31 January 2020
26/48	LS8-OLI/TIRS	9 May 2020
26/48	LS8-OLI/TIRS	19 September 2020

Once the raw images were obtained, image band analysis was done, through which the image could be organized in such a way that unique and current information could be extracted. We used the natural color compound with a combination of red (4), green (3), and blue (2) bands; see Figure 2. This approximates what human eyes see: while healthy vegetation is green, unhealthy flora is brown. Urban features appear in white and gray, water is dark blue or black, and the combinations of bathymetric bands (4, 3, 1) use red (4) and green (3), with coastal bands peaking in the water. The coastal band is helpful in coastal, bathymetric, and aerosol studies because it reflects blues and violets.

A source tile dataset was formed in ArcGIS 10.7.1 for each generated image set. A mosaic dataset was derived from managing the entire collection, and finally, the reference tile dataset was obtained to apply the final scenarios (Figure 3). The problems of data management were concerned with merging different geographical areas and resolutions.

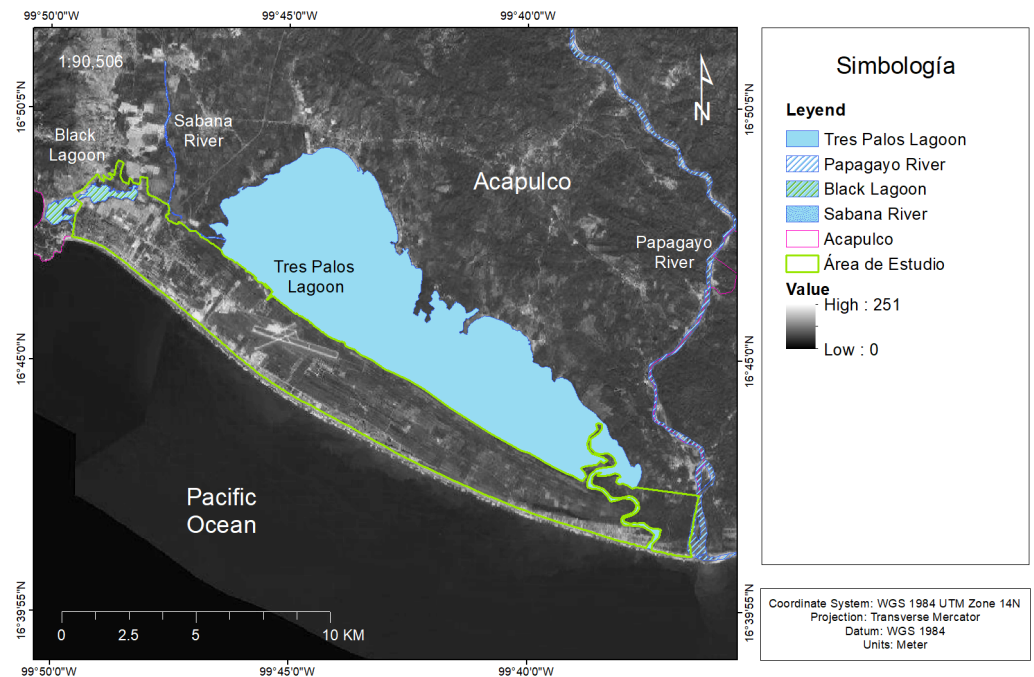
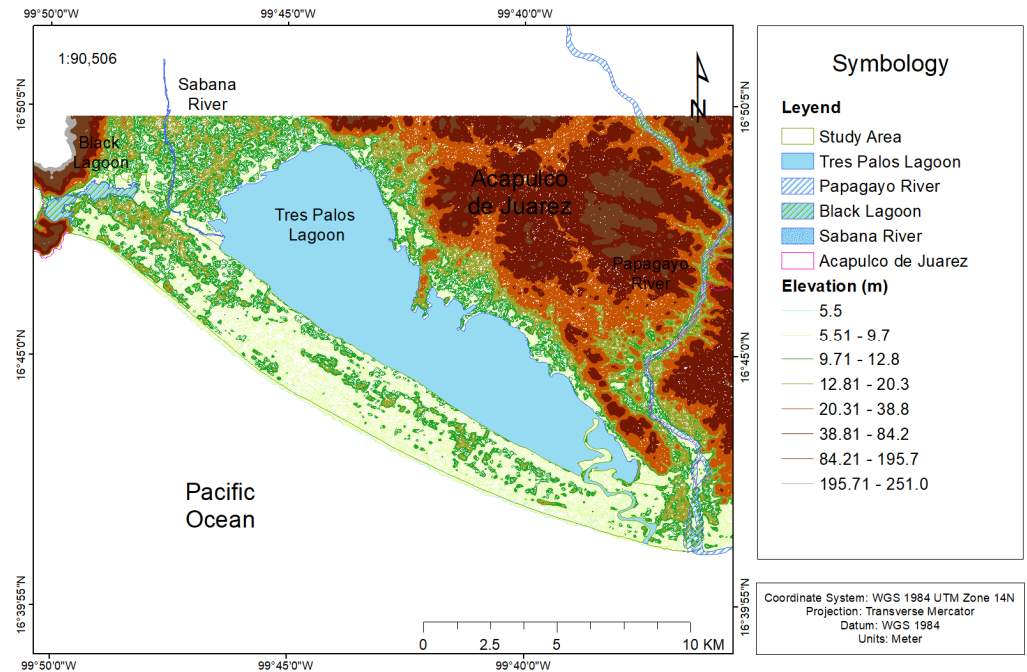


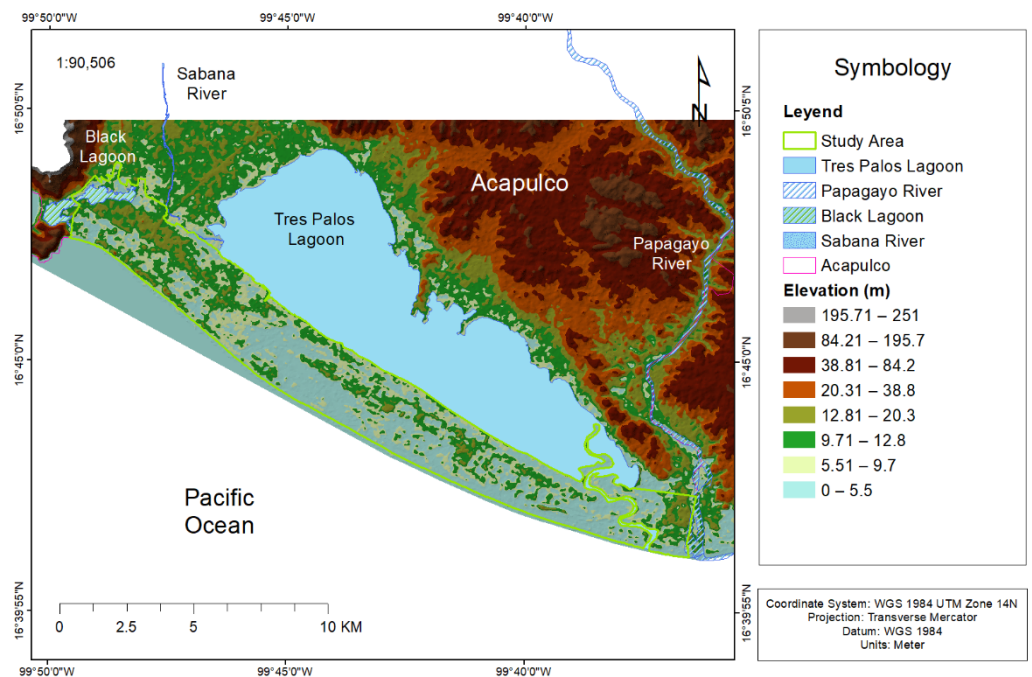
Figure 3. The raster dataset was created from several raster datasets arranged in a mosaic.

Once the mosaic data were obtained, a series of contour lines was created in Global Mapper 20 from the terrain grid. In this way, equally spaced contour lines were generated at intervals that were as small as possible from the elevation grid data entered into ArcGIS (10 cm). However, we also experimented with distances between 5 m and 1 cm, with more significant and lesser degrees of success. Next, the terrestrial LiDAR point cloud was processed on a contour map (Figure 4A).



(A)

Figure 4. Cont.



(B)

Figure 4. (A) Contour lines generated in the Global Mapper 20 program, with a height of 10 cm each. (B) Triangular irregular network (TIN) generated in ArcGIS 10.7.1 for the study area.

ArcGIS 10.7.1 used contour lines to build a triangulated irregular network (TIN). The TIN components were constructed from vector data, which represent surface features. Once the TIN was created, geoprocessing tools were used to add additional vector data, thus generating a network of streams and delineating watersheds; see Figure 4B. In situ data were required and were collected during May 2018 and May 2019 in the Diamante Zone to validate the modeling. Through seven field visits made to different villages within the study area (Figure 5), empirical terrain data (in situ) were obtained with GPS receivers, which allowed us to estimate a negative bias on the average vertical axis of -5.7 m.

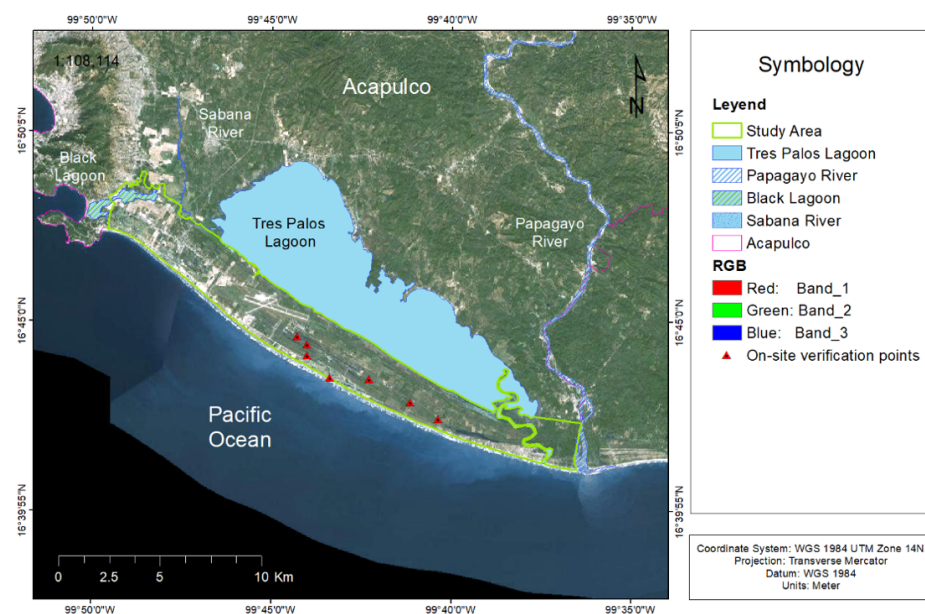


Figure 5. In red, the seven height measurements made with GPS are indicated to validate the altimetric information of the digital elevation model.

INEGI's cartographic maps show a resolution 4.53175 m below that obtained with our raster, which we have used as the digital elevation model. Therefore, a "manual" adjustment was made in the database; this adjustment consisted of subtracting the value of 4.53175 m from the minimum elevation value of each layer in INEGI. In the maps herein, said error was eliminated. Once the TIN was obtained with additional hydrography data, we transformed the resulting layer into a raster by interpolation. ArcGIS assigns each output cell a height, or a value without information, depending on whether the center of the cell falls within the TIN interpolation zone or not (Figure 6). The output raster more accurately represents the TIN surface; since the raster has a cell structure, it cannot maintain the edges of the thick and thin cutting lines present in the TIN [63].

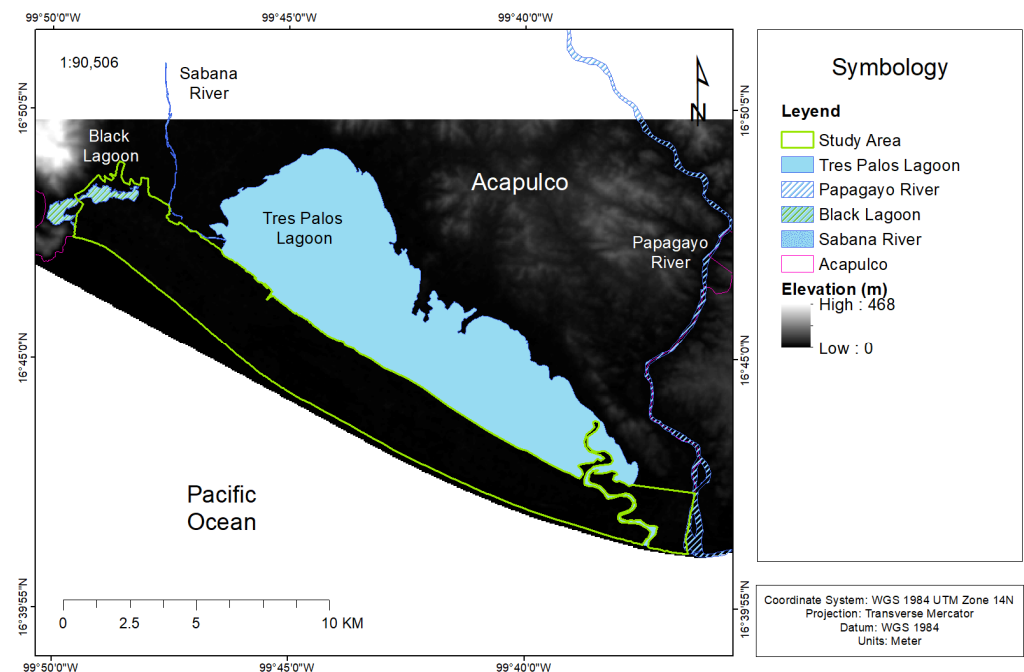


Figure 6. Raster image generated in ArcGIS through triangular irregular network interpolation (TIN).

A sensitivity analysis was applied to the resolution of the generated raster through three sets of simulations. The raster images were generated for sensitivity analysis with spatial resolutions of 10 m, 20 m, and 50 m [63]. The bilinear interpolation method generated the images using a weighted average of the four closest cell centers. The closer the input cell to the center of the output cell, the greater the influence of its value on the value of the output cell. This means that the output value may differ from the nearest input's, but it is always within the same range of values as the input [64].

Once the final raster was obtained, this public image was cropped with the shapefile of the specific study area of the Diamante Zone. The horizontal resolution of the elevation data is one arcsecond, which corresponds to approximately 50 m. The maps reflect land elevations relative to extreme coastal water levels and do not incorporate potential defenses such as levees.

The territory of the study area was classified into three main types to assess land use (Figure 7):

1. Agricultural area (cultivated land, livestock production, and aquaculture);
2. Urban area (residential, recreation, culture, wholesale warehouse, commercial building, business, financial services, market, and plant nursery);
3. Natural resource areas (bodies of water, mangrove, xerophilous scrub, and low deciduous forest).

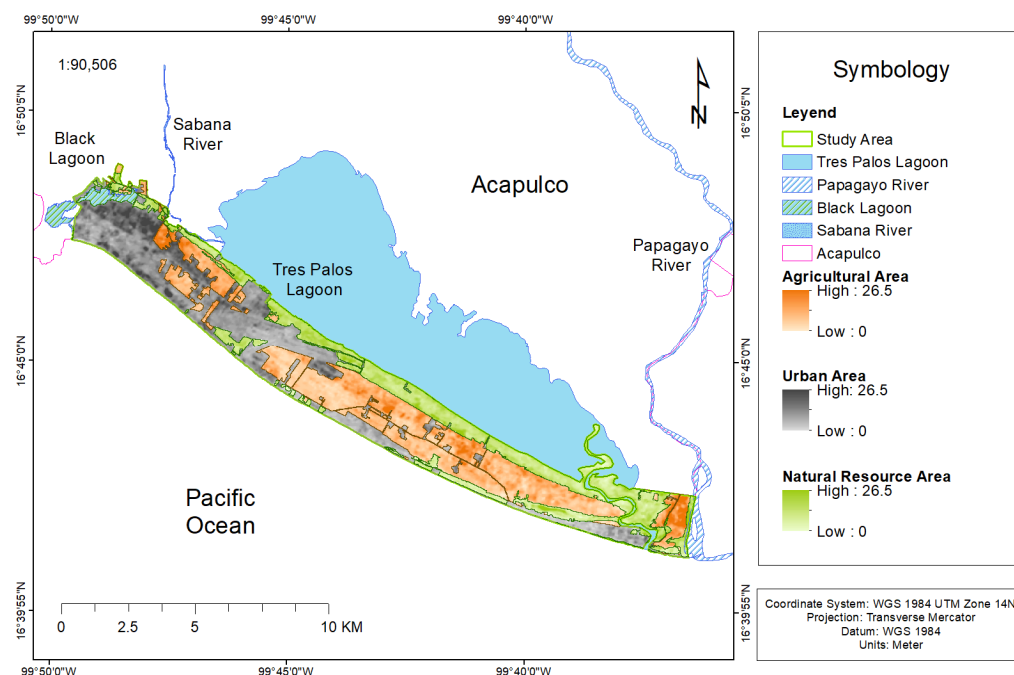


Figure 7. Map showing the types of habitats based on the official land uses in the study area. Identification of the habitat type in the study area: Agricultural Area, Urban Area, and Natural Resource Area. All interior polygons were dissolved, and a mask of the digital elevation model was cut to create three individual rasters.

The impacts of coastal flood risk on agricultural, urban, and natural resource areas were mapped. The impacts of flooding on each of the habitat types identified in the study area were classified into the scenarios Optimistic SSP1-RCP2.6, Conservative SSP2-RCP4.5, or Extremist SSP5-RCP8.5; see Figure 7.

Historical observed and reconstructed water levels are used to establish the relationship between flood probability and flood height. Altitude data refer to the mean sea level in the datum WGS 1984 UTM Zone 14N [65]. A cartographic database was also used to identify deltaic areas related to bodies of water (such as seas, rivers, lagoons). The habitat of Acapulco Diamante was classified according to Corine's land cover map [66]. In addition to coastal flooding, the study area is also vulnerable to surface water flooding due to its low topography, intense rainfall episodes during the season of floods and tropical storms, and the low level of drainage capacity [67].

3. Results

In this discussion, we consider the uncertainties in the global sea level scenarios, such as the loss of ice from Greenland and Antarctica, due to ocean circulation, for example, which has been widely discussed by [56]. Figure 8C, Figure 9C, and Figure 10C show the three prospective scenarios chosen for this study as products of global warming due to climate change: (9c) Optimistic SSP1-RCP2.6, (10c) Conservative SSP2-RCP4.5, and (11c) Extremist SSP5-RCP8.5. Each image shows the maximum flood level for each scenario chosen for 2081–2100.

The areas designated as Null are those that will not be affected by flooding caused by the increase in sea level as a result of climate change until the period 2081–2100. The possibility that these areas may be flooded in subsequent time periods is beyond the scope of this study and will require further analysis of the data.

Along most coasts, local sea level changes can differ by 20% or more from the global mean change, coupled with the effects of long-period tides, and this can significantly increase the frequency of a given extreme water level [68]. To calculate the percentage and area of flooding, each of the scenarios shown in Figure 8 used a manual solution. This

consisted of creating a database showing the pixel counts of classes containing each of the break values in which the digital elevation model was classified; for the present study, these are 2041–2060, 2061–2080, and 2081–2100 (see Table 4). As already mentioned, in our digital elevation model, each pixel represents an area of 50 m × 50 m above the ground [59].

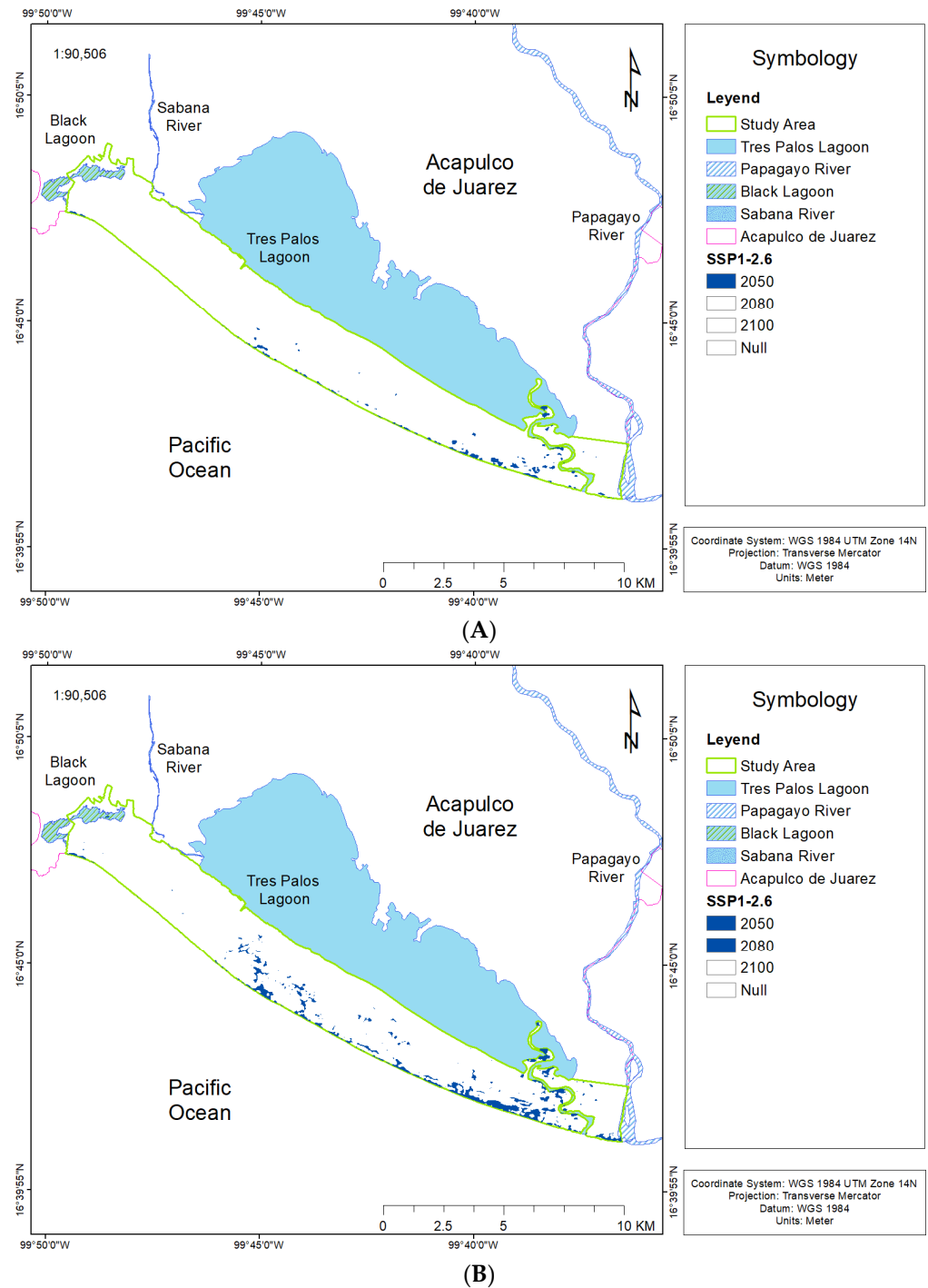


Figure 8. Cont.

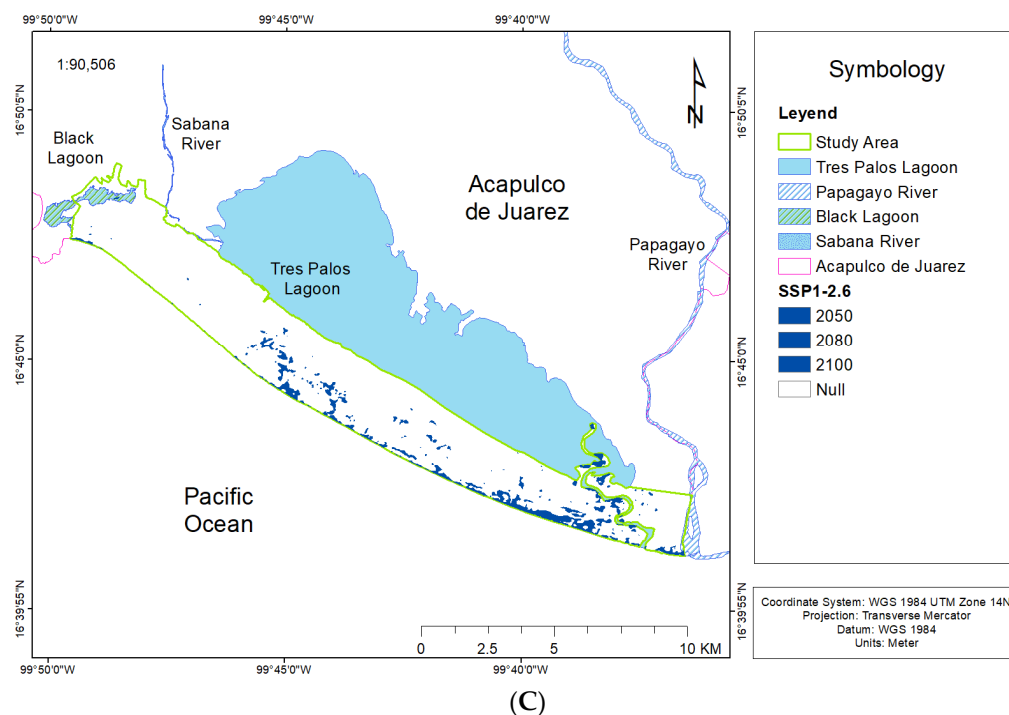


Figure 8. Prospective flooding caused by sea level rise based on SSP1-RCP2.6, for (A) 2041–2060, (B) 2061–2080, and (C) 2081–2100.

Table 4. Percentage and area (km²) that could be underwater, in scenarios (A) Optimistic SSP1-RCP2.6, (B) Conservative SSP2-RCP4.5, and (C) Extremist SSP5-RCP8.5.

Optimistic SSP1-2.6			
Year	Percentage	Area (km ²)	
2041–2060	1	21,717	(A)
2061–2080	5	78,040	
2081–2100	7	109,787	
Conservative SSP2-RCP4.5			
Year	Percentage	Area (km ²)	
2041–2060	1	21,717	(B)
2061–2080	11	169,550	
2081–2100	19	294,030	
Extremist SSP5-RCP8.5			
Year	Percentage	Area (km ²)	
2041–2060	1	21,717	(C)
2061–2080	24	370,265	
2081–2100	35	540,320	

Acapulco Diamante’s total flood zone is likely to increase by approximately 22 km² between 2041 and 2060, based on the current coastline, from the boundary of the official Federal Maritime Land Zone for the municipality of Acapulco [54]—a rise of 0.54 m—and by approximately 540 km² for the period 2081–2100 due to a local sea level rise of 2.67 m, compared to the average values for 1995–2014 (Table 4). A local sea level rise would have repercussions such as frequent road closures, reduced stormwater drainage capacity, deteriorating infrastructure, and saltwater intrusion into drinking water extraction wells. In turn, this would have socioeconomic consequences that would impact restaurant businesses by the sea, tourism service companies, fishing, and many other areas. This point forces us to consider future political plans to mitigate these urban effects.

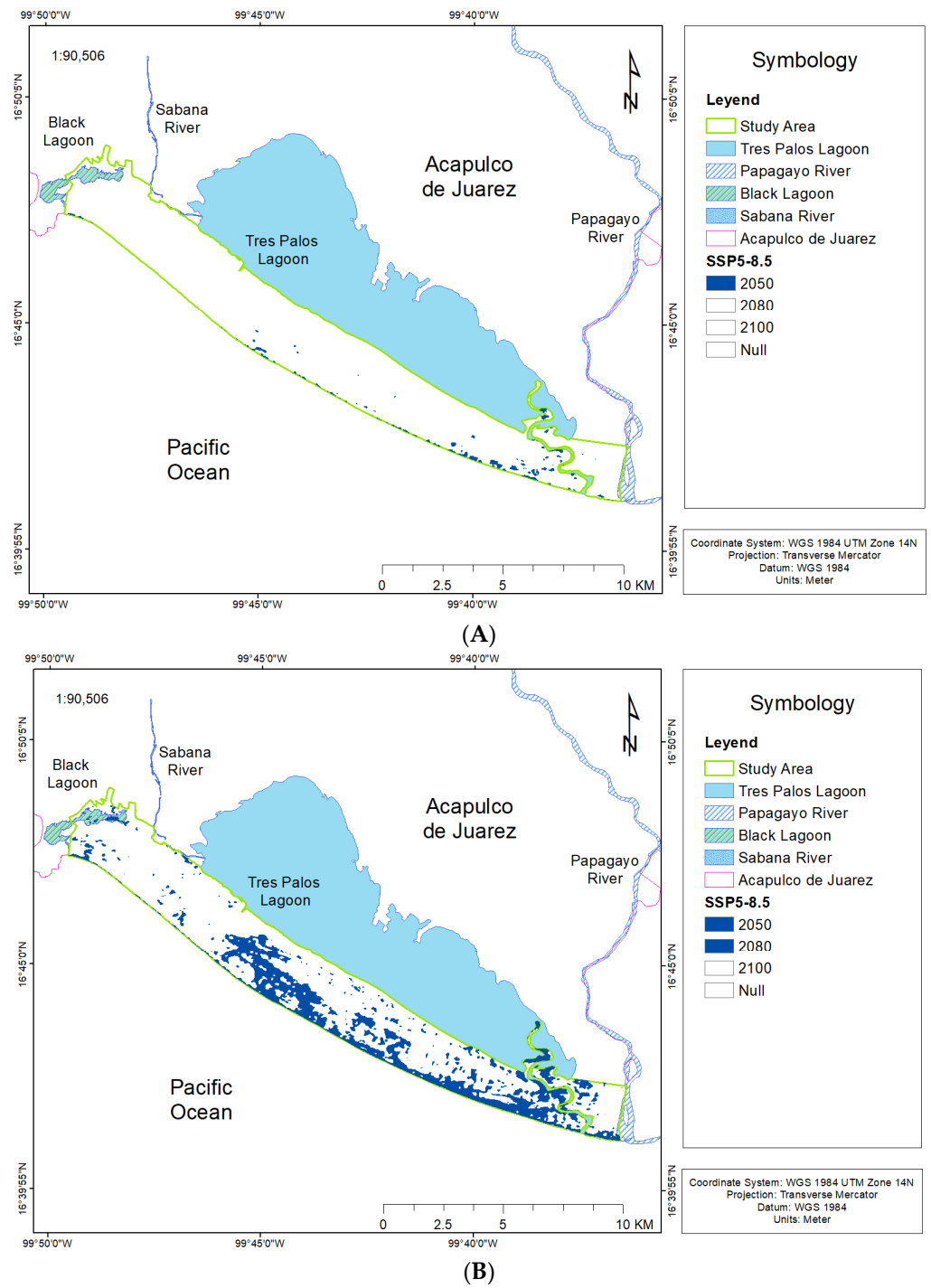


Figure 9. Cont.

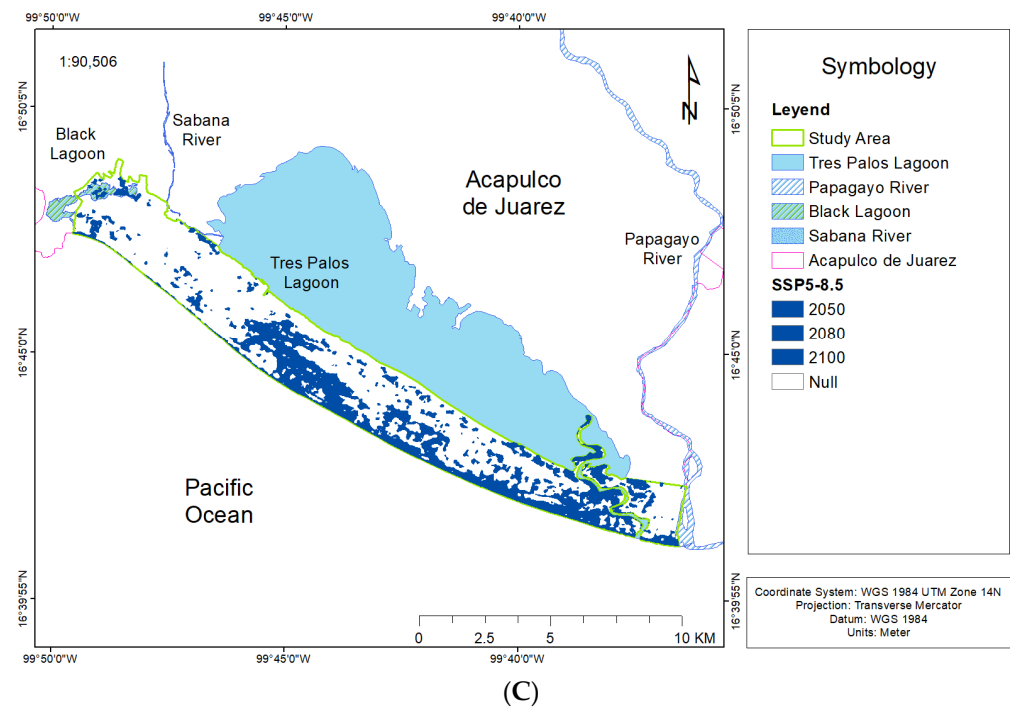
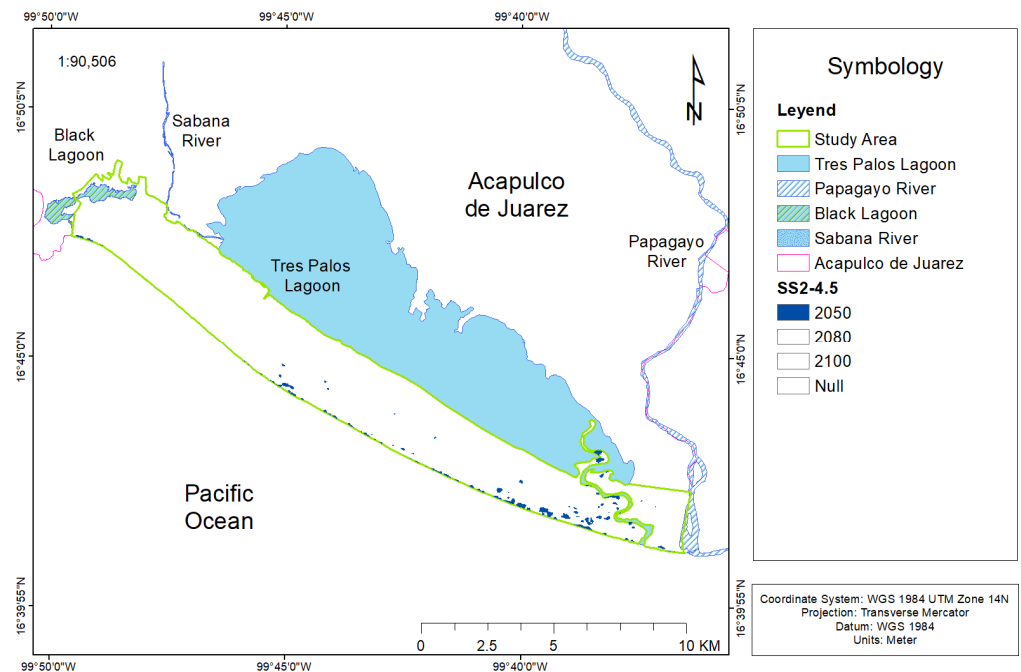


Figure 9. Flood forecast related to sea level rise based on SSP5-8.5, for (A) 2041–2060, (B) 2061–2080, and (C) 2081–2100.

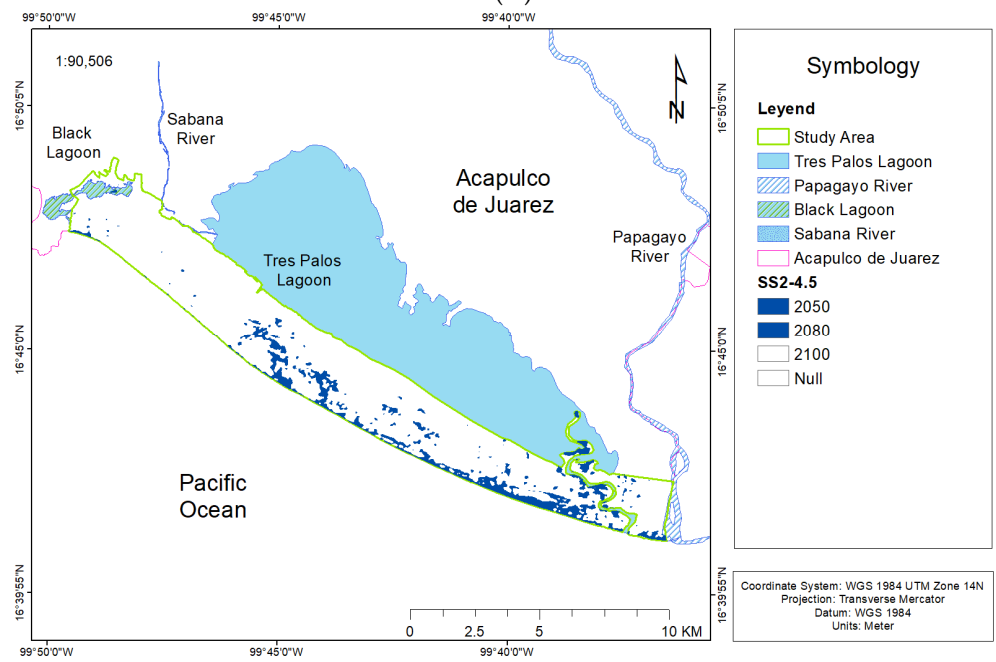
The results show that the percentage of urban area affected by possible flooding in the SSP1-RCP2.6 scenario would increase from 2% in 2041–2060 to 8% in 2081–2100 (see Table 5 and Figure 8), and the percentage of urban area affected by the SSP5-8.5 scenario would increase from 2% to 32% in the same period (see Table 6 and Figure 9).

Table 5. Flood area percentages for the scenario Optimistic SSP1-RCP2.6 with the three land uses: (A) agricultural area, (B) urban area, and (C) natural resources area.

Year	Percentage	Area (km ²)	
2041–2060	1	3208	(A)
2061–2080	4	22,145	
2081–2100	6	32,860	
Null	94	532,945	
Total	100	565,805	
Year	Percentage	Area (km ²)	
2041–2060	2	11,360	(B)
2061–2080	6	33,375	
2081–2100	8	44,595	
Null	92	535,345	
Total	100	579,940	
Year	Percentage	Area (km ²)	
2041–2060	1	6165	(C)
2061–2080	6	24,263	
2081–2100	8	33,643	
Null	92	383,443	
Total	100	417,085	



(A)



(B)

Figure 10. Cont.

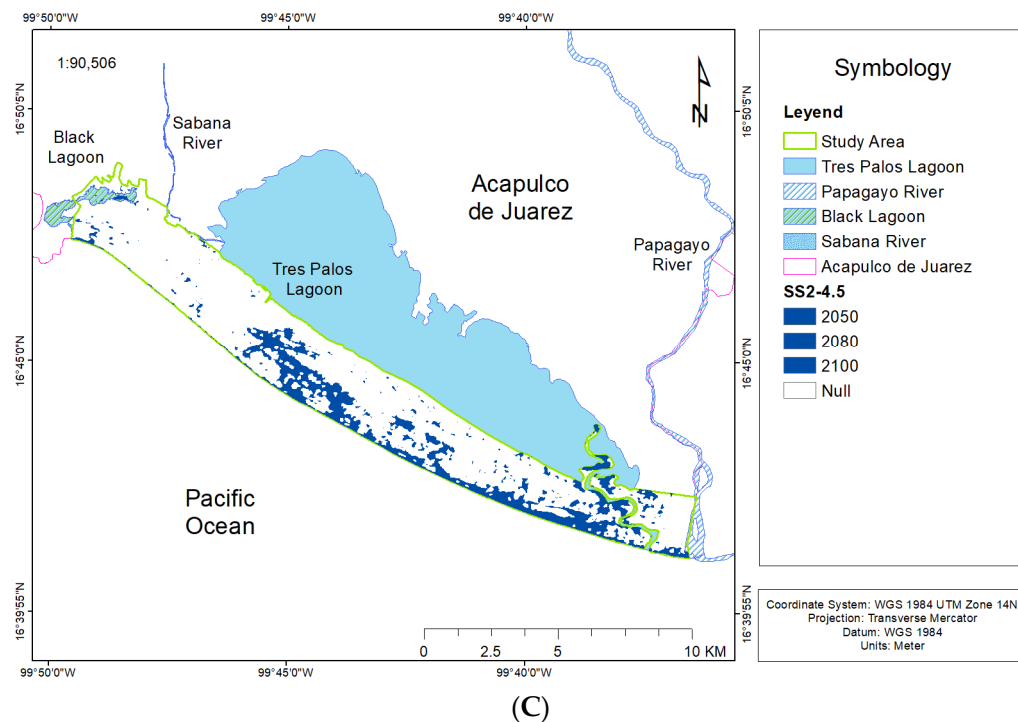


Figure 10. Prospective flooding by sea level rise based on SSP2-RCP4.5 by (A) 2041–2060, (B) 2061–2080, and (C) 2081–2100.

Table 6. Percentages of flood area for the Extremist scenario SSP5-RCP8.5 under the three land uses: (A) agricultural area, (B) urban area, and (C) resource area.

Year	Percentage	Area (km ²)	
2041–2060	1	3705	(A)
2061–2080	25	138,760	
2081–2100	34	193,165	
Null	66	372,640	
Total	100	565,805	
Year	Percentage	Area (km ²)	
2041–2060	2	11,360	(B)
2061–2080	23	134,125	
2081–2100	32	187,795	
Null	68	392,145	
Total	100	579,940	
Year	Percentage	Area (km ²)	
2041–2060	2	7200	(C)
2061–2080	24	101,255	
2081–2100	36	152,195	
Null	64	264,890	
Total	100	417,085	

The percentage of the agricultural area that will be affected by 2081–2100 will be approximately 20%, compared to the 1% forecast for 2041–2060, under the SSP2–4.5 scenario, which can be attributed to the greater flood area in 2081–2100 compared to 2041–2060; see Table 7 and Figure 10. Agricultural zone flood rates in future scenarios increase significantly the closer we get to 2081–2100; under the SSP5–8.5 scenario, the percentage of flooding in the period 2041–2060 is only 1%, but for 2081–2100, it is an alarming 34%; see Table 6 and Figure 9.

Table 7. Percentages and flood areas for the Conservative scenario SSP2-RCP4.5: (A) agricultural area, (B) urban area, and (C) natural resources area.

Year	Percentage	Area (km ²)	
2041–2060	1	3705	
2061–2080	10	54,058	(A)
2081–2100	20	112,760	
Null	80	453,045	
Total	100	565,805	
Year	Percentage	Area (km ²)	
2041–2060	2	11,360	
2061–2080	11	64,458	(B)
2081–2100	19	108,838	
Null	81	471,103	
Total	100	579,940	
Year	Percentage	Area (km ²)	
2041–2060	2	7200	
2061–2080	12	49,525	(C)
2081–2100	18	76,513	
Null	82	340,573	
Total	100	417,085	

4. Discussion

Globally, decision makers and resource managers will be challenged to preserve existing urban and natural habitats. As the first major tourist city on the Mexican Pacific, Acapulco is a representative coastal city. Impacts associated with sea level rise worsen flooding of coastal communities during severe hydrometeorological events and promote erosion, loss of coastal dunes, and loss of habitats.

Through the use of the coastal flood maps generated through the IPESLI method during this study, policy makers can begin to prioritize appropriate responses to future inundation from sea level rise. By providing local elevation values and formulating a time frame in which the greatest impacts of sea level rise inundation may manifest themselves, policy makers can begin to formulate long-term adaptation strategies beyond the current 15-year planning horizon.

The IPESLI procedure proposed here estimated with a high degree of accuracy (above 85%) the prospective effects of sea level rise in a coastal area, since the flood zone showed 87% consistency with water level data. Our method is versatile since satellite images make the remote study possible under non-stationary conditions, particularly in situations such as the pandemic, which has been unfolding since 2019. This allows minimizing field visits in situ. At the same time, it is a comparatively fast, and therefore low-cost, method. A corporation or an academic institution can acquire satellite images that are not freely accessible and can thus substantially improve the data quality.

However, as demonstrated, it is not always necessary for databases to be adjusted with a high degree of accuracy. This could allow this method to be used in other areas where local data on the effect of climate change on the coastal zone are lacking. This will allow for the better calibration and validation of existing models that deal with coastal flooding phenomena, whether they are the product of climate change or are only temporary.

This study has used scenarios supported by sea level rise projections constructed by Kopp et al. (2017) [31]. These scenarios bear relevance for political decision making at the local level, since they foresee the need for adaptation by estimating, in advance, the retreat of coasts on mainlands and islands of low altitude, which will be very vulnerable during the second half of the 21st century. Creating a shared framework of vital information on sea level rise is essential for better supporting stakeholders, and especially coastal decision makers.

Incorporating climate change science, and specifically the science around sea level rise, into the updating of existing laws and the creation of new public policy is challenging [69]. Providing information with spatial data and imagery can help reduce personal discretion in decision making by public administrators [70]. In the context of coastal planning, it has been suggested that a top-down approach with the presence of strong leadership is the best way to eliminate discretion [71].

A few international research projects have focused on risk management and adaptation, specifically designed for small-scale coastal zones, where satellite images have been used to generate maps showing expected sea level rise levels. An increase of about 25% in inundation area is expected by 2100 in the central region of Singapore [72]. By 2070–2080, the Bengal tiger is expected to have lost the entirety of its natural habitat in the Sundarbans mangrove forest in southwestern Bangladesh [73]. Depending on the RCP-SSP projection, an inundation area in San Francisco Bay of between 90 and 218 km² is expected [74]. Entire coastal dune habitats worldwide are expected to be reduced as a result of permanent sea level rise [75]. The Guadeloupe area is expected to present future chronic flooding and severe impacts given the high urbanization [76]. The results of our study represent a step in the right direction with respect to the lack of spatial information for sea level rise projections for the Mexican South Pacific coast. These types of studies increase the awareness of the community that will have to deal with permanent increases in the coastal strip, which will lead them to implement new adaptation strategies to cope with potential future economic, natural, and cultural impacts. Therefore, this analysis provides a new tool for public administrators to monitor and evaluate at-risk areas in order to prevent the loss of property and potentially future human lives.

The simulated flood magnitudes related to local sea level rise may be overestimated because future structural flood control measures have not been considered (since there are none) and also because of the micro details of the topography in the model's configuration. In addition, the above results should be considered in the context of implicit error. Factors such as buildings, vegetation, terrain slope, and random noise can cause vertical errors in elevation data, leading to the incorrect classification of areas as safe or risky. Different elevation data sources also contain errors, both in their typical range and in their average.

In subsequent studies, an analysis of morphological conditions (estuary areas, retro-dune areas, old emissaries of the lagoon filled up, etc.) is recommended. For example, in the case of the Acapulco Diamante coast, the role of the lagoon's emissary cannot be denied.

5. Conclusions

This article concludes that, if the increase in global temperature stops at 2 °C in relation to 1850–1900, it is possible that, by 2081–2100, up to 5% of the study area will be affected by extreme floods, leading to approximately 78 km² of flooded land. If we reach 3 °C, 24% of the zone could be flooded (approximately 371 km²), and it could be 35% if we reach 5.7 °C, representing up to 541 km² of flooded land. Future research may exclude several scenarios that cannot be ruled out today. However, the effects of local subsidence may continue to contribute to future relative sea level changes in some areas, and these need to be characterized. To determine the regional consequences of global phenomena such as global warming, the constant and systematic monitoring of phenomena such as sea level increases is required.

The IPESLI procedure presents a proof-of-concept for a policy-making tool designed to graphically show the impact that sea level rise could have on a low-elevation coastal area. The methodology allows high quality estimates to be achieved, while, at the same time, it is applicable to all coastal areas of the planet, taking into account that its cost-benefit is relatively low in relation to the available data and resources. The coastal inundation maps created in this study can be used to identify the most vulnerable areas and initiate decision making that will benefit both wetland and coastal areas, as well as nearby communities, and should be taken into account for conscious land-use planning and the creation of climate adaptation strategies.

Although the exercise is still perfectible, and improvements can always be made, the present procedure has the potential to contribute to forming a communication bridge between climate change science and local decision makers, which will contribute to moving sea level rise adaptation in the right direction. Implementing this type of methodology through citizen science initiatives such as observatories could account for the constant evolution of projections for this problem. In the same way, it would make visible a problem that has been little discussed in the local and national public spheres due to our perceived remoteness from the consequences of these phenomena.

Author Contributions: Conceptualization, R.S.G.-V. and E.A.G.C.; Data curation, R.S.G.-V., A.T.-M. and A.C.C.Á.; Formal analysis, R.S.G.-V., A.T.-M. and A.C.C.Á.; Funding acquisition, R.S.G.-V.; Investigation, R.S.G.-V. and M.I.R.V.; Methodology, R.S.G.-V. and M.R.U.; Project administration, R.S.G.-V., A.T.-M. and J.L.R.-A.; Resources, R.S.G.-V., A.T.-M., A.C.C.Á. and M.R.U.; Software, R.S.G.-V. and M.R.U.; Supervision, A.T.-M.; Validation, A.T.-M. and A.C.C.Á.; Visualization, R.S.G.-V.; Writing—original draft, R.S.G.-V.; Writing—review & editing, R.S.G.-V., A.T.-M., A.C.C.Á., M.R.U., J.L.R.-A., M.I.R.V. and E.A.G.C. All authors have read and agreed to the published version of the manuscript.

Funding: This research received no external funding.

Institutional Review Board Statement: Not applicable.

Informed Consent Statement: Not applicable.

Data Availability Statement: Not applicable.

Conflicts of Interest: The authors declare no conflict of interest.

References

1. IPCC. *The Ocean and Cryosphere in a Changing Climate*; Cambridge University Press: Cambridge, UK, 2019. [CrossRef]
2. Haasnoot, M.; Kwadijk, J.; van Alphen, J.; Le Bars, D.; van den Hurk, B.; Diermanse, F.; van der Spek, A.; Essink, G.O.; Delsman, J.; Mens, M. Adaptation to uncertain sea-level rise; how uncertainty in Antarctic mass-loss impacts the coastal adaptation strategy of the Netherlands. *Environ. Res. Lett.* **2020**, *15*, 034007. [CrossRef]
3. IPCC. *Climate Change 2021: The Physical Science Basis*; Cambridge University Press: Cambridge, UK, 2021; Volume AR6.
4. IPCC. *Global Warming of 1.5 °C*; Cambridge University Press: Cambridge, UK, 2018; Volume 2.
5. IPCC. *Climate Change 2007: The Physical Science Basis*; Solomon, S., Qin, D., Manning, M., Chen, Z., Marquis, M., Averyt, K.B., Tignor, M., Miller, H.L., Eds.; Cambridge University Press: Cambridge, UK, 2007.
6. NASA How Much Rise Should We Expect from Greenland and Antarctica? Available online: <https://sealevel.nasa.gov/faq/11/how-much-rise-should-we-expect-from-greenland-and-antarctica/> (accessed on 14 January 2022).
7. Colleoni, F.; Naish, T.; De Conto, R.; De Santis, L.; Whitehouse, P. The Uncertain Future of Antarctica's Melting Ice. *EOS* **2022**, *103*, 503. [CrossRef]
8. IPCC. *Climate Change 2014: Impacts, Adaptation, and Vulnerability. Part B: Regional Aspects*; Barros, V.R., Field, C.B., Dokken, D.J., Mastrandrea, M.D., Mach, K.J., Bilir, T.E., Chatterjee, M., Ebi, K.L., Estrada, Y.O., Genova, R.C., et al., Eds.; Cambridge University Press: Cambridge, UK, 2014; Volume 25.
9. IPCC. *Sea Level Rise and Implications for Low-Lying Islands, Coasts and Communities*; Cambridge University Press: Cambridge, UK, 2019; Volume 4.
10. Hinkel, J.; Church, J.A.; Gregory, J.M.; Lambert, E.; Le Cozannet, G.; Lowe, J.; McInnes, K.L.; Nicholls, R.J.; Pol, T.D.; Wal, R. Meeting User Needs for Sea Level Rise Information: A Decision Analysis Perspective. *Earth's Future* **2019**, *7*, 320–337. [CrossRef]
11. NASA Regional Relative Sea-Level Change. Available online: <https://sealevel.nasa.gov/understanding-sea-level/regional-sea-level/overview> (accessed on 14 January 2022).
12. Gómez-Villeras, R.S.; Galán Castro, E.A.; Ruz Vargas, M.I. Activismo ambiental e incidencia para la adaptación al cambio climático en Acapulco. *Espiral Estud. Sobre Estado Soc.* **2021**, *28*, 291–398. [CrossRef]
13. Rahmstorf, S. A Semi-Empirical Approach to Projecting Future Sea-Level Rise. *Science* **2007**, *315*, 368–370. [CrossRef]
14. Mastrandrea, M.D.; Mach, K.J.; Plattner, G.-K.; Edenhofer, O.; Stocker, T.F.; Field, C.B.; Ebi, K.L.; Matschoss, P.R. The IPCC AR5 guidance note on consistent treatment of uncertainties: A common approach across the working groups. *Clim. Chang.* **2011**, *108*, 675–691. [CrossRef]
15. Burcharth, H.F.; Lykke Andersen, T.; Lara, J.L. Upgrade of coastal defence structures against increased loadings caused by climate change: A first methodological approach. *Coast. Eng.* **2014**, *87*, 112–121. [CrossRef]
16. Gilbert, S.; Horner, R. *The Thames Barrier*; Thomas Telford Ltd.: London, UK, 1986; ISBN 0727702491.
17. Wilby, R.L.; Nicholls, R.J.; Warren, R.; Wheeler, H.S.; Clarke, D.; Dawson, R.J. Keeping nuclear and other coastal sites safe from climate change. *Proc. Inst. Civ. Eng. Civ. Eng.* **2011**, *164*, 129–136. [CrossRef]

18. Hino, M.; Field, C.B.; Mach, K.J. Managed retreat as a response to natural hazard risk. *Nat. Clim. Chang.* **2017**, *7*, 364–370. [[CrossRef](#)]
19. Bienvenido-Huertas, D.; Rubio-Bellido, C.; Marín-García, D.; Canivell, J. Influence of the Representative Concentration Pathways (RCP) scenarios on the bioclimatic design strategies of the built environment. *Sustain. Cities Soc.* **2021**, *72*, 103042. [[CrossRef](#)]
20. van Vuuren, D.P.; Edmonds, J.; Kainuma, M.; Riahi, K.; Thomson, A.; Hibbard, K.; Hurtt, G.C.; Kram, T.; Krey, V.; Lamarque, J.-F.; et al. The representative concentration pathways: An overview. *Clim. Chang.* **2011**, *109*, 5–31. [[CrossRef](#)]
21. Riahi, K.; van Vuuren, D.P.; Kriegler, E.; Edmonds, J.; O'Neill, B.C.; Fujimori, S.; Bauer, N.; Calvin, K.; Dellink, R.; Fricko, O.; et al. The Shared Socioeconomic Pathways and their energy, land use, and greenhouse gas emissions implications: An overview. *Glob. Environ. Chang.* **2017**, *42*, 153–168. [[CrossRef](#)]
22. Tebaldi, C.; Debeire, K.; Eyring, V.; Fischer, E.; Fyfe, J.; Friedlingstein, P.; Knutti, R.; Lowe, J.; O'Neill, B.; Sanderson, B.; et al. Climate model projections from the Scenario Model Intercomparison Project (ScenarioMIP) of CMIP6. *Earth Syst. Dyn.* **2021**, *12*, 253–293. [[CrossRef](#)]
23. Kebede, A.S.; Nicholls, R.J.; Allan, A.; Arto, I.; Cazarro, I.; Fernandes, J.A.; Hill, C.T.; Hutton, C.W.; Kay, S.; Lázár, A.N.; et al. Applying the global RCP–SSP–SPA scenario framework at sub-national scale: A multi-scale and participatory scenario approach. *Sci. Total Environ.* **2018**, *635*, 659–672. [[CrossRef](#)]
24. Turnpenny, J.; Haxeltine, A.; O'Riordan, T. A Scoping Study of User Needs for Integrated Assessment of Climate Change in the UK Context: Part 1 of the Development of an Interactive Integrated Assessment Process. *Integr. Assess.* **2004**, *4*, 283–300. [[CrossRef](#)]
25. Kulp, S.; Strauss, B.H. Rapid escalation of coastal flood exposure in US municipalities from sea level rise. *Clim. Chang.* **2017**, *142*, 477–489. [[CrossRef](#)]
26. McMichael, C.; Dasgupta, S.; Ayeb-Karlsson, S.; Kelman, I. A review of estimating population exposure to sea-level rise and the relevance for migration. *Environ. Res. Lett.* **2020**, *15*, 123005. [[CrossRef](#)]
27. Dasgupta, S.; Laplante, B.; Meisner, C.; Wheeler, D.; Yan, J. The impact of sea level rise on developing countries: A comparative analysis. *Clim. Chang.* **2009**, *93*, 379–388. [[CrossRef](#)]
28. Cooper, H.M.; Fletcher, C.H.; Chen, Q.; Barbee, M.M. Sea-level rise vulnerability mapping for adaptation decisions using LiDAR DEMs. *Prog. Phys. Geogr. Earth Environ.* **2013**, *37*, 745–766. [[CrossRef](#)]
29. Lentz, E.E.; Thieler, E.R.; Plant, N.G.; Stippa, S.R.; Horton, R.M.; Gesch, D.B. Evaluation of dynamic coastal response to sea-level rise modifies inundation likelihood. *Nat. Clim. Chang.* **2016**, *6*, 696–700. [[CrossRef](#)]
30. Gold, M. *D2.1 EU Citizen Observatories Landscape Report—Frameworks for Mapping Existing CO Initiatives and Their Relevant Communities and Interactions*, 1st ed.; Wehn, U., See, L., Moorthy, I., Domian, D., Eds.; ECSA: Berlin, Germany, 2018.
31. Kopp, R.E.; DeConto, R.M.; Bader, D.A.; Hay, C.C.; Horton, R.M.; Kulp, S.; Oppenheimer, M.; Pollard, D.; Strauss, B.H. Evolving Understanding of Antarctic Ice-Sheet Physics and Ambiguity in Probabilistic Sea-Level Projections. *Earth's Future* **2017**, *5*, 1217–1233. [[CrossRef](#)]
32. Muis, S.; Verlaan, M.; Winsemius, H.C.; Aerts, J.C.J.H.; Ward, P.J. A global reanalysis of storm surges and extreme sea levels. *Nat. Commun.* **2016**, *7*, 11969. [[CrossRef](#)]
33. Solorio Sandoval, I.F.; Carrillo Jiménez, A.R.; Guzmán Gómez, I.M. La arquitectura institucional de la política climática de México: Un análisis desde el enfoque de integración de políticas. *Estud. Políticos* **2020**, *51*, 191–216. [[CrossRef](#)]
34. Solorio, I.; Ortega, J.; Romero, R.; Guzmán, J. AMLO's populism in Mexico and the framing of the extractivist agenda: The construction of the hegemony of the people without the indigenous voices. *Zeitschrift für Vergleichende Politikwissenschaft* **2021**, *15*, 249–273. [[CrossRef](#)]
35. ICAP. *Mexico*; International Carbon Action Partnership: Berlin, Germany, 2021.
36. Godinho, C.; Coetzee, K. *Climate Transparency Report 2020*; Goodman, T., Ed.; Climate Transparency: Berlin, Germany, 2020; Volume 53, ISBN 9788578110796.
37. INEGI. *Cuaderno Estadístico Acapulco de Juárez, Guerrero*; INEGI: Aguascalientes, Mexico, 2006.
38. INEGI. *Panorama Sociodemográfico de México*; INEGI: Aguascalientes, Mexico, 2021; Volume 49.
39. INEGI. *Cuaderno Estadístico Municipal: Acapulco de Juárez, Guerrero*; de Guerrero, G.d., de Juárez, A.d., Eds.; Instituto Nacional de Estadística Geografía e Informática: Aguascalientes, Mexico, 1999; ISBN 9701328787.
40. Valderrama-Landeros, L.; Rodríguez-Zúñiga, M.; Troche-Souza, C.; Velázquez-Salazar, S.; Villeda-Chávez, E.; Alcántara-Maya, J.; Vázquez-Balderas, B.; Cruz-López, M.; Ressler, R. *Manglares de México: Actualización y exploración de los datos del sistema de monitoreo 1970/1980–2015*; Comisión Nacional para el Conocimiento y Uso de la Biodiversidad: Ciudad de México, Mexico, 2017; p. 128. ISBN 978-607-8328-78-9.
41. Cárdenas Gómez, E.P. Crecimiento y planeación urbana en Acapulco, Cancún y Puerto Vallarta (México). *Rev. Investig. Tur.* **2016**, *99*–120. [[CrossRef](#)]
42. INEGI. *Principales Resultados del Censo de Población y Vivienda 2010*; INEGI: Aguascalientes, Mexico, 2011; Volume 1.
43. H. Ayuntamiento de Acapulco de Juárez. *Plan Director Urbano de la Zona Metropolitana de Acapulco de Juárez, Guerrero*; Secretaría de Gobernación, Secretaría del Medio Ambiente Recursos Naturales y Pesca, Secretaría de la Reforma Agraria, Secretaría de Comunicaciones y Transporte, Comisión Nacional del Agua, Comisión para la Regulación de la Tenencia de la Tierra, Eds.; H. Ayuntamiento Municipal de Acapulco de Juárez: Acapulco de Juárez, Mexico, 2001.

44. González-González, J.; Salmeron-Gallardo, Y.; Torres-Espino, G.; Reyes-Umaña, M.; Sampedro-Rosas, M.L.; Rojas-Herrera, A. Análisis de riesgo en cauces y estaciones sub-eléctricas en AGEB's de la zona 07, Acapulco, Guerrero. In *Calidad Ambiental y Desarrollo Sustentable: Tomo III*; Rosas, M.L.S., Acevedo, J.L.R., López, A.L.J., Eds.; Servicios Editoriales Especializados: Toluca, Mexico, 2014; pp. 200–214.
45. Rodríguez-Herrera, A.L.; Ruz-Vargas, M.I.; Hernández-Rodríguez, B. Riesgo y vulnerabilidad en Llano Largo, Acapulco: La tormenta Henriette. *Econ. Soc. Territ.* **2012**, *7*, 425–447. [[CrossRef](#)]
46. Matías-Ramírez, L.G. Algunos efectos de la precipitación del huracán Paulina en Acapulco, Guerrero. *Investig. Geogr.* **1998**, *1*, 7–20. [[CrossRef](#)]
47. Flores-Lorenzo, P.; Dávila-Hernández, N. Mapeo de áreas inundadas utilizando imágenes de radar TanDEM-X en Acapulco de Juárez, Guerrero-México. *Terra Digit.* **2018**, *2*. [[CrossRef](#)]
48. Pasch, R.J.; Zelinsky, D.A. *Hurricane Manuel*; EP132013; NOAA: Honolulu, HI, USA, 2013.
49. Rivera González, O.D. Colapso de la red de drenaje y repercusiones urbanas en la zona costera de Acapulco, México, derivados de la tormenta tropical Manuel, 2013–2020. *Estud. Socioterritoriales Rev. Geogr.* **2020**, *28*, 62. [[CrossRef](#)]
50. SECTUR. Sector Vulnerabilidad del Destino Turístico Acapulco. In *Estudio de la Vulnerabilidad y Programa de Adaptación Ante la Variabilidad Climática y el Cambio Climático en Diez Destinos Turísticos Estratégicos, Así Como Propuesta de un Sistema de Alerta Temprana a Eventos Hidrometeorológicos Extremos*; SECTUR: Cuernavaca, Mexico, 2014; p. 31.
51. Zavala-Hidalgo, J.; de Buen-Kalman, R.; Romero-Centeno, R.; Hernández-Maguey, F. Tendencias del nivel del mar en las costas mexicanas. In *Vulnerabilidad de la Zonas Costeras Mexicanas Ante el Cambio Climático*; Botello, A.V., Villanueva-Fragoso, S., Gutiérrez, J., Rojas Galaviz, J.L., Eds.; SEMARNAT-INE, y UNAM-ICMYL: Ciudad de México, Mexico, 2010; pp. 249–268. ISBN 9786077887119.
52. UN HABITAT. *Cities and Climate Change: Policy Directions Global Report on Human Settlements 2011*; Abridged; Earthscan: London, UK, 2011; ISBN 9789211319293.
53. SEDESOL. *Atlas de Peligros Naturales de la Ciudad y Puerto de Acapulco de Juárez. Guerrero*; SEDESOL: Acapulco de Juárez, Mexico, 2009.
54. Kopp, R.E.; Horton, R.M.; Little, C.M.; Mitrovica, J.X.; Oppenheimer, M.; Rasmussen, D.J.; Strauss, B.H.; Tebaldi, C. Probabilistic 21st and 22nd century sea-level projections at a global network of tide-gauge sites. *Earth's Future* **2014**, *2*, 383–406. [[CrossRef](#)]
55. Hinkel, J.; Jaeger, C.; Nicholls, R.J.; Lowe, J.; Renn, O.; Peijun, S. Sea-level rise scenarios and coastal risk management. *Nat. Clim. Chang.* **2015**, *5*, 188–190. [[CrossRef](#)]
56. Jevrejeva, S.; Frederikse, T.; Kopp, R.E.; Le Cozannet, G.; Jackson, L.P.; van de Wal, R.S.W. Probabilistic Sea Level Projections at the Coast by 2100. *Surv. Geophys.* **2019**, *40*, 1673–1696. [[CrossRef](#)]
57. Pattyn, F. The paradigm shift in Antarctic ice sheet modelling. *Nat. Commun.* **2018**, *9*, 2728. [[CrossRef](#)]
58. NASA IPCC AR6 Sea Level Projection Tool. Available online: <https://sealevel.nasa.gov/ipcc-ar6-sea-level-projection-tool> (accessed on 14 January 2022).
59. USA Geological Survey USGS Earth Explorer. Available online: <https://earthexplorer.usgs.gov/> (accessed on 17 September 2020).
60. INEGI; INE; CONAGUA. *Cuencas Hidrográficas de México*; Comisión Nacional para el Conocimiento y Uso de la Biodiversidad: Ciudad de México, Mexico, 2007.
61. INEGI. *Modelos Digitales de Elevación: Generalidades y Especificaciones*, 1st ed.; Instituto Nacional de Estadística Geografía e Informática: Aguascalientes, Mexico, 1999; ISBN 970-13-2511-7.
62. USA Geological Survey Landsat 8-9 Operational Land Imager (OLI) and Thermal Infrared (TIRS) Collection 2 Level-2 Science Products 30-meter multispectral data. Available online: <https://doi.org/10.5066/F71835S6> (accessed on 13 February 2020).
63. McCoy, J.; Johnston, K.; Kopp, S.; Borup, B.; Willison, J.; Payne, B. Using ArcGIS Spatial Analyst. *Esri* **2002**, *380*, 238.
64. Esri El Tamaño de la Celda y el Remuestreo en Análisis. Available online: <https://desktop.arcgis.com/es/arcmap/10.3/guide-books/extensions/spatial-analyst/performing-analysis/cell-size-and-resampling-in-analysis.htm> (accessed on 8 January 2019).
65. EPSG WGS 84/UTM zone 14N. Available online: <https://epsg.io/32614> (accessed on 1 September 2021).
66. Balzter, H.; Cole, B.; Thiel, C.; Schmuilius, C. Mapping CORINE Land Cover from Sentinel-1A SAR and SRTM Digital Elevation Model Data using Random Forests. *Remote Sens.* **2015**, *7*, 14876–14898. [[CrossRef](#)]
67. Rodríguez-Herrera, A.L. *Las Inundaciones en Llano Largo, Acapulco: Riesgo, Turismo y Desarrollo*; Plaza y Valdés: Madrid, Spain, 2011; ISBN 9786074022803.
68. Church, J.A.; Clark, P.U.; Cazenave, A.; Gregory, J.M.; Jevrejeva, S.; Levermann, A.; Merrifield, M.A.; Milne, G.A.; Nerem, S.; Nunn, P.D.; et al. Sea Level Change. In *Climate Change 2013: The Physical Science Basis. Contribution of Working Group I to the Fifth Assessment Report of the Intergovernmental Panel on Climate Change*; Stocker, T.F., Qin, D., Plattner, G.-K., Tignor, M., Allen, S.K., Boschung, J., Nauels, A., Xia, Y., Bex, V., Midgley, P.M., Eds.; Cambridge University Press: Cambridge, UK, 2013; pp. 1137–1216. ISBN 978-1-107-66182-0.
69. Keys, N.; Bussey, M.; Thomsen, D.C.; Lynam, T.; Smith, T.F. Building adaptive capacity in South East Queensland, Australia. *Reg. Environ. Chang.* **2014**, *14*, 501–512. [[CrossRef](#)]
70. Morrison, T.H. Developing a regional governance index: The institutional potential of rural regions. *J. Rural Stud.* **2014**, *35*, 101–111. [[CrossRef](#)]
71. Schmidt, P.; Morrison, T.H. Watershed management in an urban setting: Process, scale and administration. *Land Use Policy* **2012**, *29*, 45–52. [[CrossRef](#)]

72. Catalao, J.; Raju, D.; Nico, G. In-sar Maps of Land Subsidence and Sea Level Scenarios to Quantify the Flood Inundation Risk in Coastal Cities: The Case of Singapore. *Remote Sens.* **2020**, *12*, 296. [[CrossRef](#)]
73. Mukul, S.A.; Alamgir, M.; Sohel, M.S.I.; Pert, P.L.; Herbohn, J.; Turton, S.M.; Khan, M.S.I.; Munim, S.A.; Reza, A.H.M.A.; Laurance, W.F. Combined effects of climate change and sea-level rise project dramatic habitat loss of the globally endangered Bengal tiger in the Bangladesh Sundarbans. *Sci. Total Environ.* **2019**, *663*, 830–840. [[CrossRef](#)]
74. Shirzaei, M.; Bürgmann, R. Global climate change and local land subsidence exacerbate inundation risk to the San Francisco Bay Area. *Sci. Adv.* **2018**, *4*, eaap9234. [[CrossRef](#)]
75. Chu, M.L.; Guzman, J.A.; Muñoz-Carpena, R.; Kiker, G.A.; Linkov, I. A simplified approach for simulating changes in beach habitat due to the combined effects of long-term sea level rise, storm erosion, and nourishment. *Environ. Model. Softw.* **2014**, *52*, 111–120. [[CrossRef](#)]
76. Le Cozannet, G.; Idier, D.; de Michele, M.; Legendre, Y.; Moisan, M.; Pedreros, R.; Thiéblemont, R.; Spada, G.; Raucoules, D.; de la Torre, Y. Timescales of emergence of chronic flooding in the major economic center of Guadeloupe. *Nat. Hazards Earth Syst. Sci.* **2021**, *21*, 703–722. [[CrossRef](#)]